AC

TIFR-EHEP/94-05
May 20, 1994

Precision Measurement of Z Boson Properties at LEP

S. Banerjee
Tata Institute of Fundamental Research, Bombay

Abstract

W and Z bosons, the carriers of electroweak interactions, were discovered in 1983 in the CERN $p\bar{p}$ collider. The Large Electron Positron collider (LEP) at CERN has made extensive study of the properties of Z boson and thereby made critical tests of the Electroweak theory and the QCD. One has also looked for yet another fundamental particle, the Higgs boson. Some of the important results from LEP have been reviewed here. Lepton universality has been tested in charged and neutral current sectors with high precision. Number of light neutrino families has been found to be 2.980 ± 0.027. Standard Model agrees with data at 0.5% level. There is indirect evidence of top quark with mass around 166 GeV. Higgs boson of mass smaller than 63.5 GeV has been ruled out at 95% confidence level in the framework of Standard Model.

Talk given at Bose and Twentieth Century Physics, Calcutta, December 1993

1 Introduction

Weak interaction as seen in the β-decays of nuclei has been well described by V−A theory as a four fermion interaction. The theory was similar to that of electromagnetic interaction and is given by a universal coupling constant G_F. However, this theory leads to a linearly rising cross section for ν-nucleon scattering with s. This prediction agrees well with experiments using highest energy ν beam but violates unitarity at cm energies $\approx$ 300 GeV. Heavy charged vector boson $W^{\pm}$ exchange was proposed to cure this bad high energy behaviour of the theory. The high energy ν data demanded m_W to be greater than 60 GeV. On the other hand, unitarity demands m_W to be less than 1500 GeV.

In the framework of the theory of weak interaction, $W^{\pm}$ is coupled to a pair of leptons $\ell^{\pm}$ ν or a pair of $q\bar{q}$ of same colour but different flavours with the same coupling strength. So in principle, one can produce $W^{\pm}$ in hadron colliders and then the $W^{\pm}$'s can be observed through their decay to a lepton pair. This idea has led Rubbia, McIntyre and Cline [1] to propose a $p\bar{p}$ collider to be built at CERN. $p\bar{p}$ collider was built at CERN operating at $\sqrt{s} \approx 540$ GeV with luminosity $\approx 10^{30}$ cm^{-2}sec^{-1}. Two hermetic detectors UA1 and UA2 were built to detect leptons and missing energies coming from the collision. The two experiments [2] observed events with large transverse energy lepton and large transverse missing energy. The plot of missing energy parallel to the lepton direction, as in figure 1 (from [3]), clearly shows a striking back-to-back configuration of the lepton-neutrino system. This established the evidence of W particles with mass $80.3^{+0.4}_{-1.3}$ GeV.

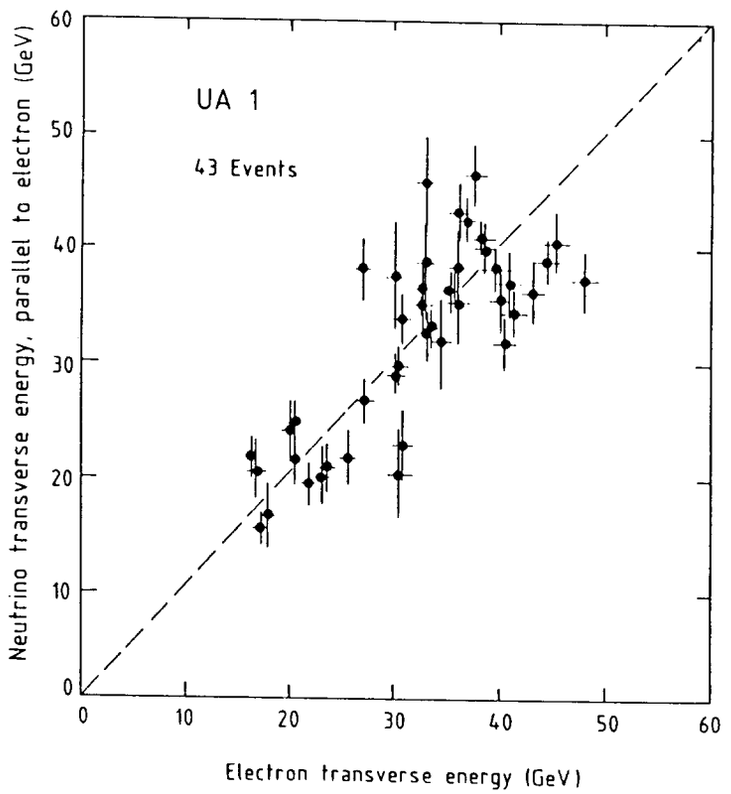

Figure 1: Correlation between the electron and neutrino transverse energies. The neutrino component along the electron direction is plotted against the electron transverse energy.

The reaction $e^+e^- \rightarrow W^+W^-$ goes via ν or γ exchange and this also violates unitarity. The

unitarity can be restored by introducing a neutral current coupled to e^+e^- as well as W^+W^-. This has led Weinberg, Salam and Glashow [4] to formulate the Standard Model unifying electromagnetic and weak interactions. This model is described by 4 vector boson fields. Two of these fields give W^+ and W^-. The remaining two fields mix to give γ and Z with the mixing angle $\sin^2\theta_W = 1 - \frac{m_W^2}{m_Z^2}$.

Again low energy ν data determine $\sin^2\theta_W$ rather precisely and in the framework of SM these measurements give an estimate of $m_Z \approx 100$ GeV. The same detectors in the $p\bar{p}$ collider [5] found events with high mass e^+e^- or $\mu^+\mu^-$ pair. The effective mass of the dilepton system peaks around 93 GeV and one estimates the mass of the Z Particles to be 93.9 ± 2.9 GeV.

2 LEP and Experiments

The Large Electron Positron collider (LEP) [6] has been built at CERN to study the properties of these W and Z bosons. This machine has been operating in Geneva since August, 1989. It is the largest instrument of its kind. It is situated in an underground tunnel of 27 km circumference in the French-Swiss border (see figure 1). The machine has been designed to operate with electron and positron beams of energy between 50-100 GeV. Over the last few years, however, LEP has been operating at cm energies around 92 GeV to study the properties of the Z boson. Later the beam energy will be upgraded to ≈ 90 GeV to study the properties of W bosons.

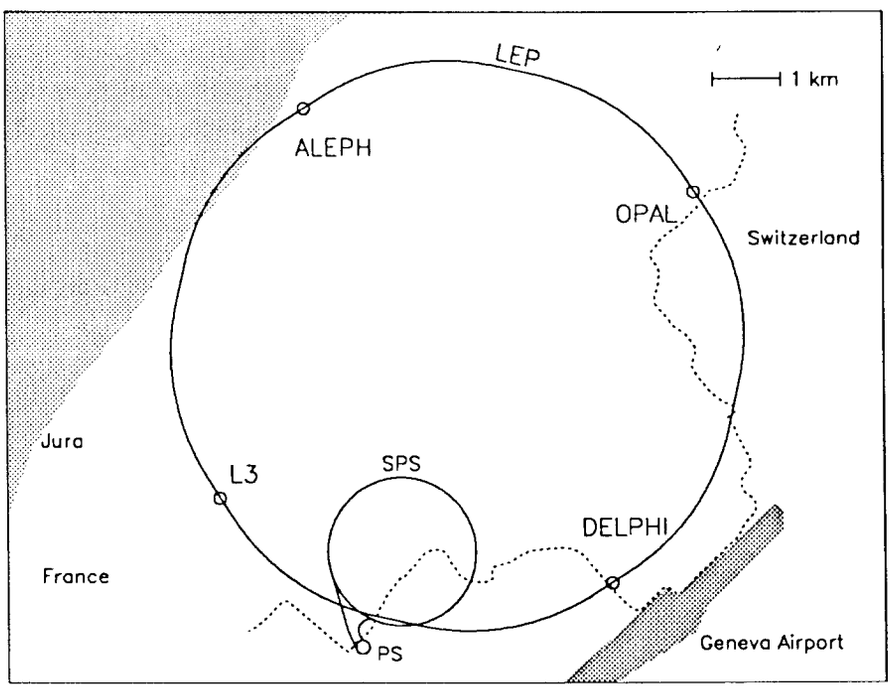

Figure 2: The LEP Collider

Four intersection regions of LEP are equipped with general purpose detectors, ALEPH, DELPHI, L3 and OPAL, to study the characteristic of all the interactions. With the high

luminosity of LEP, each of the 4 experiments collected over 1 million Z events during this period. Figure 3 shows the integrated luminosity seen by the experiments from 1990 to 1992. The integrated luminosity (delivered by LEP to each of the 4 detectors) has grown from 6 pb^{-1} in 1990 to 13, 22 and 32 pb^{-1} over the next 3 years. The large number of events could reduce the statistical errors significantly.

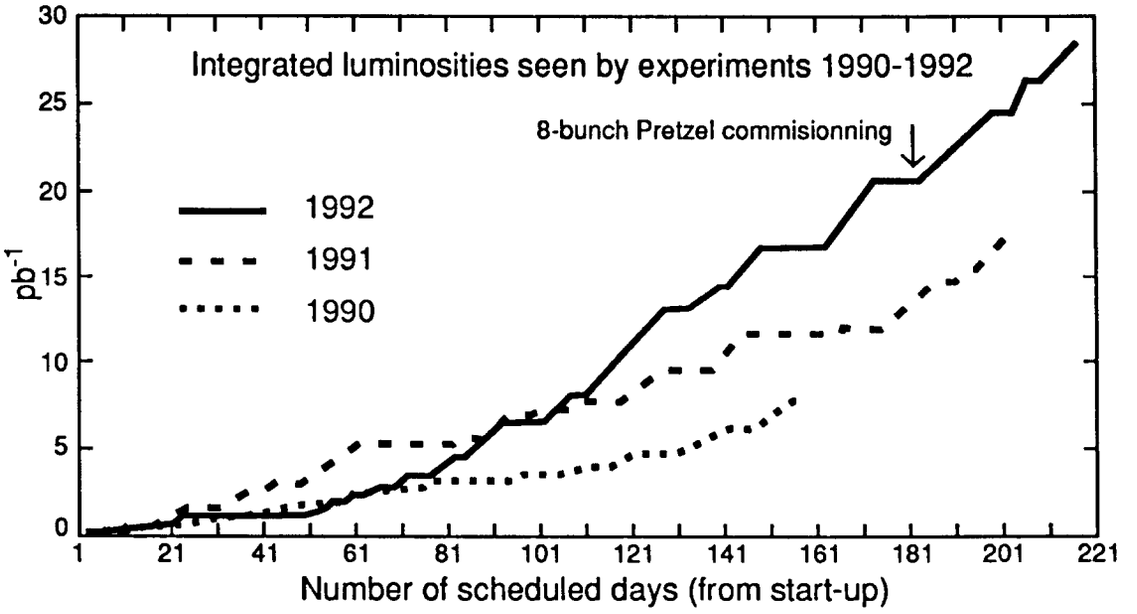

Figure 3: Integrated luminosity seen by the LEP experiments from 1990 to 1992

Each experiment utilizes a combination of tracking devices in solenoidal magnetic field and calorimeters. The goal is to detect and measure electron, muon and photon energy and direction precisely. The detectors also measure energy flow of hadrons coming from the interactions. Typical examples of events seen by the LEP detectors are given in figure 4.

3 Electroweak Parameters

The electroweak parameters are obtained from the following experimental measurements :

- Cross section as a function of cm energy $\sqrt{s}$
- Forward-backward asymmetry of charged leptons at different cm energies
- Polarization asymmetry of τ lepton
- Cross section and asymmetry for tagged quark flavour

3.1 Theoretical Prediction

The basic process involved in all these processes is fermion pair production through γ and Z exchanges. In the lowest order electroweak theory [4], the cross section for the process $e^+e^- \to f\bar{f}$ is expressed as a sum of 3 terms : γ exchange, Z exchange and γ-Z interference. For $e^+e^- \to e^+e^-$, t-channel exchange of γ/Z is possible and hence there will be additional terms due to interference of s-t amplitudes. Basic couplings are between γ and $f\bar{f}$ of strength $-iq_f\gamma^\mu$, and between Z and $f\bar{f}$ of strength $-i\frac{g}{\cos\theta_W}\gamma^\mu\frac{g_{vf}-g_{af}\gamma^5}{2}$. Here we denote

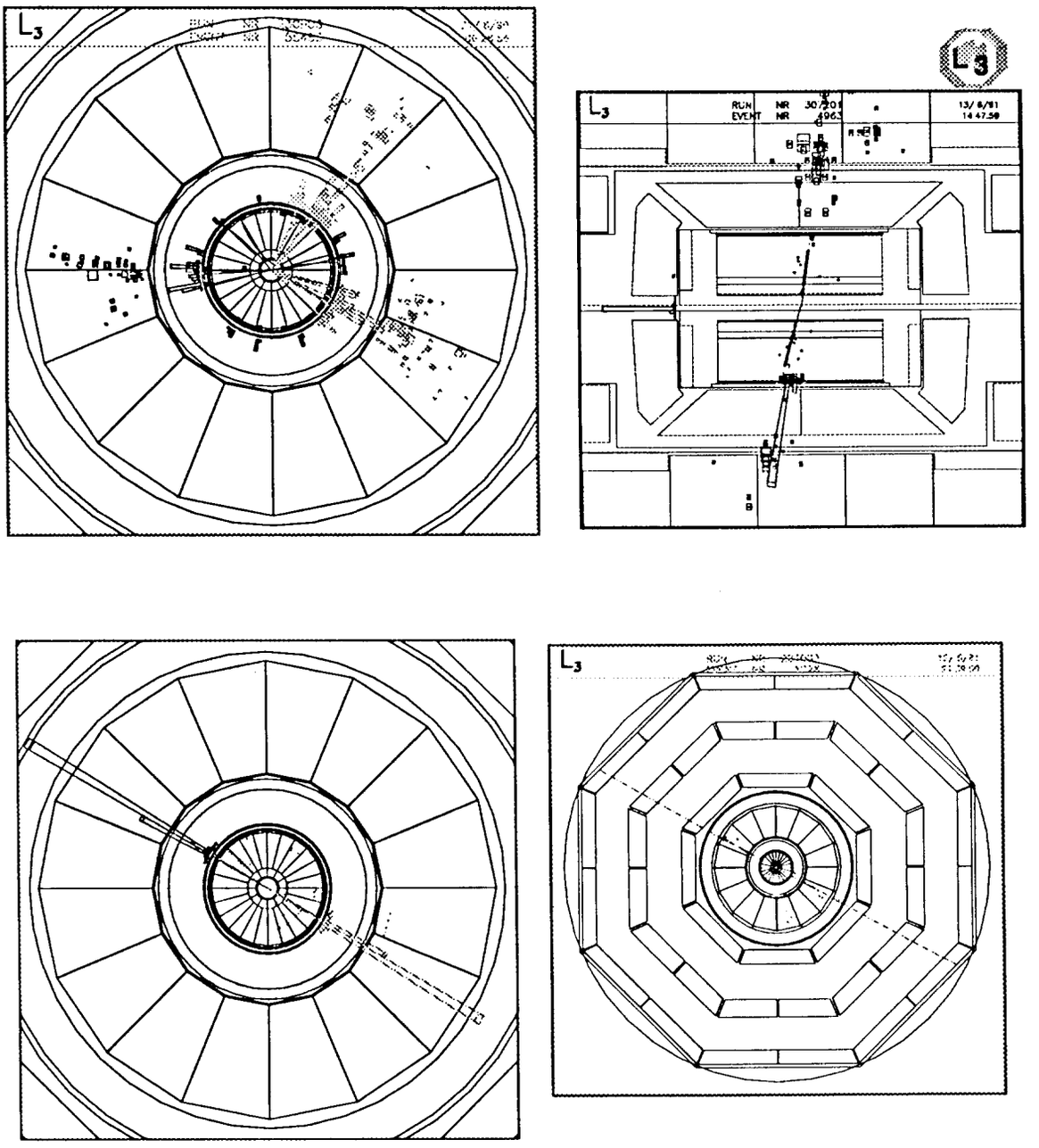

Figure 4: Examples of Z decaying to $q\bar{q}g$, $\tau^+\tau^-$, e^+e^-, $\mu^+\mu^-$ final states

$$
\begin{aligned}
q_f &= \text{charge of fermion} \\
g_{vf} &= I_3^f - 2q_f \sin^2\theta_W \qquad \text{(vector coupling)} \\
g_{af} &= I_3^f \qquad \text{(axial vector coupling)} \\
I_3^f &= \text{weak isospin of fermion}
\end{aligned}
$$

This leads to a simplified expression for cross section

$$\sigma^0(s) = \sigma_Z^0 + \sigma_\gamma^0 + \sigma_{\gamma Z}^0$$

where

$$
\begin{aligned}
\sigma_Z^0 &= \frac{12\pi}{m_Z^2}\frac{\Gamma_e\Gamma_f}{\Gamma_Z^2}\frac{s\Gamma_Z^2}{(s-m_Z^2)^2+m_Z^2\Gamma_Z^2} \\
\sigma_\gamma^0 &= \frac{4\pi\alpha^2}{3s}q_f^2 N_C^f \\
\sigma_{\gamma Z}^0 &= \frac{2\sqrt{2}\alpha}{3}(q_f G_F N_C^f g_{ve} g_{vf})\frac{(s-m_Z^2)m_Z^2}{(s-m_Z^2)^2+m_Z^2\Gamma_Z^2} \\
\Gamma_f &= \text{partial width of } Z \to f\bar{f} \\
&= \frac{G_F m_Z^3}{6\sqrt{2}\pi}\left(g_{vf}^2 + g_{af}^2\right) N_C^f
\end{aligned}
$$

The lowest order expressions given above must be corrected for electroweak and QCD radiative effects [7]. The electroweak corrections can be divided into two parts

- QED corrections, which take into account real photon bremsstrahlung and virtual photon loops. These corrections depend strongly on details of the experimental cuts but are largely independent of the detailed structure of the underlying electroweak theory. These corrections are large and require careful treatment. The largest contribution to this is due to initial state radiation.

- Weak corrections, which involve vector boson propagator corrections, vertex corrections and box diagrams with at least one vector boson exchanged. These corrections are not very sensitive to the experimental cuts, but strongly depend on the detailed structure of the electroweak theory. The corrections are medium-large around Z mass and have complex structure.

The corrections due to initial state radiation are taken into account by convoluting the cross section $\hat{\sigma}$ (corrected for other photonic and weak contributions) with a radiator function, H(x,s), which signifies the probability of radiating fraction x of total cm energy in the initial state.

$$\sigma(s) = \int_0^{x_{max}} H(x,s)\,\hat{\sigma}[s(1-x)]\,dx$$

The cross section term $\hat{\sigma}$ is computed at a reduced cm energy. The radiator function has been calculated to complete second order with soft photon exponentiation.

Other photonic and weak corrections are incorporated by replacing the bare couplings with effective couplings. So one measures the effective couplings of Z

$$
\begin{aligned}
\bar{g}_a &= \sqrt{\bar{\rho}}\, I_3 \\
\bar{g}_v &= \sqrt{\bar{\rho}}\left(I_3 - 2q\sin^2\theta_{eff}\right)
\end{aligned}
$$

3.2 Experimental Measurements

To measure the cross section, events are classified from general event characteristics into one of the following categories

$$\begin{aligned} e^+e^- &\rightarrow \text{hadrons} \\ &\rightarrow e^+e^- \\ &\rightarrow \mu^+\mu^- \\ &\rightarrow \tau^+\tau^- \end{aligned}$$

Luminosity is measured by counting number of small angle Bhabha events. Correcting the number of events observed from detector acceptance, trigger bias and selection efficiency, one can determine the cross section of a given process as a function of cm energy. This gives rise to a bell shaped distribution as shown in figure 5. The peak position determines m_Z, the height

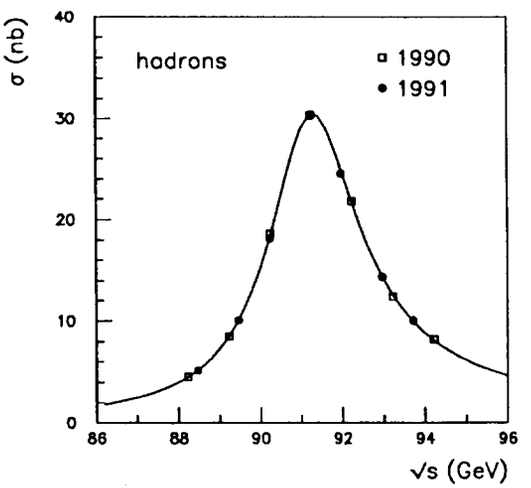

Figure 5: Hadronic cross section as a function of cm energy as seen by the L3 experiment

determines the product of initial and final state partial widths $\Gamma_e \cdot \Gamma_f$ and the width determines Γ_Z.

To obtain the forward backward asymmetry of the charged leptons, one measures the angle of the final state fermion with respect to the electron direction. An example of such an angular distribution is shown in figure 6. The angular distribution clearly shows an asymmetry between forward and backward directions and is fitted using

$$\frac{d\sigma}{d\cos\theta} \sim \left[\frac{3}{8}(1+\cos^2\theta) + A_{FB}\cos\theta\right]$$

Forward backward asymmetry is due to interference of vector and axial vector couplings of Z. At the Z pole, one can approximate

$$A_{FB}^{\ell}(m_Z^2) \simeq \frac{3}{4}A_e A_f$$

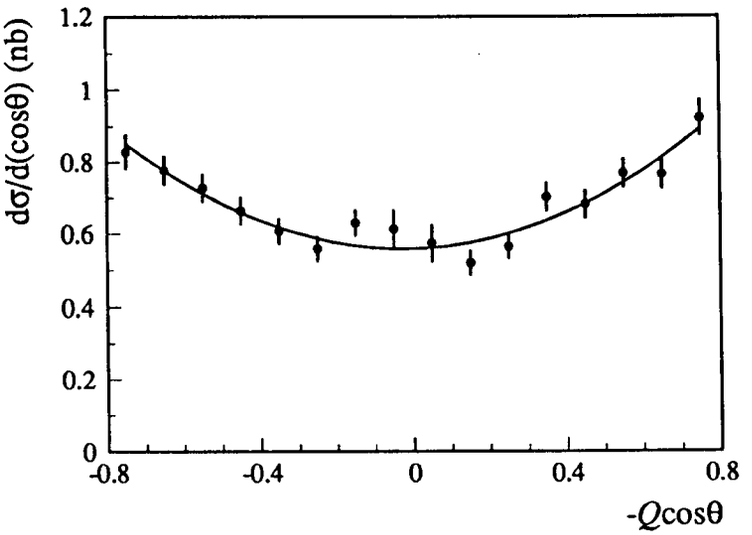

Figure 6: Angular distribution for the process $e^+e^- \to \mu^+\mu^-$ at $\sqrt{s} = 91.2$ GeV as seen by the L3 experiment at LEP

$$A_f = \frac{2g_{vf}g_{af}}{g_{vf}^2 + g_{af}^2}$$

The process Z decaying to a pair of fermions does not conserve C and P symmetries. As a result, the produced fermions are polarized longitudinally. This means that the number of fermions with helicity $\frac{1}{2}$ (spin parallel to the momentum vector) is different from those with helicity $-\frac{1}{2}$ (spin antiparallel to the momentum vector). This asymmetry has its origin in $Zf\bar{f}$ coupling. Produced Z's are polarized as well because of Ze^+e^- coupling (initial state) with polarization given by [8]

$$P_Z = -\frac{2g_{ve}g_{ae}}{g_{ve}^2 + g_{ae}^2}$$

So in principle one can measure four observables consisting of total cross section and three asymmetries

$$\begin{aligned}
\sigma_{tot} &\sim \left(g_{ve}^2 + g_{ae}^2\right)\left(g_{vf}^2 + g_{af}^2\right) \\
A_{FB} &= \frac{\sigma(\cos\theta > 0) - \sigma(\cos\theta < 0)}{\sigma_{tot}} \sim \frac{3}{4}P_Z P_f \\
A_{Pol} &= \frac{\sigma(h > 0) - \sigma(h < 0)}{\sigma_{tot}} \sim P_f \\
A_{FB}^{Pol} &= \frac{\sigma(h \cdot \cos\theta > 0) - \sigma(h \cdot \cos\theta < 0)}{\sigma_{tot}} \sim \frac{3}{4}P_Z \\
\text{with } P_f &= -\frac{2g_{vf}g_{af}}{g_{vf}^2 + g_{af}^2}
\end{aligned}$$

In the case of τ lepton production, P_τ can be deduced from an analysis of the kinematics of the τ decay products. The (V−A) helicity structure of the weak charged current decay

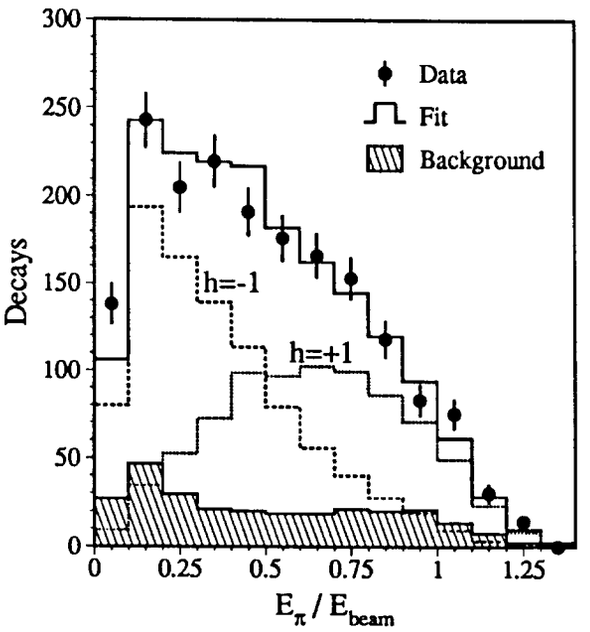

Figure 7: The spectrum of $\tau \to \pi\nu$ decays as a function of E_π as measured by L3.

leads to characteristic differences in the angular distributions in the τ rest frame, or equivalently, in the laboratory frame, to differences between the energy distributions from τ leptons of opposite helicities. LEP experiments have measured τ polarization from its leptonic and semileptonic decays. Figure 7 shows energy spectrum of the π's from τ decays compared to expected distributions from τ's with helicity ± 1.

Due to the hard fragmentation of the heavy quarks the resulting hadrons (with the corrsponding heavy flavour quantum number) carry a large fraction of the initial quark momentum, the remainder being taken up by softer hadronic particles. The heavy quark decays via the weak charged current. In case of semileptonic decays, there will be a high momentum charged lepton and missing energy due to the undetected neutrino. Due to the high mass of the heavy quark the products of the heavy hadron decay have a large transverse momentum with respect to the initial parton direction. So one can tag heavy flavour decays of Z by looking for high momentum lepton with large transverse momentum with respect to the closest hadronic jet. Choosing suitable cuts in measured momentum, p, and transverse momentum, $p_\perp$ of the leptons, one can get ~85% pure $b\bar{b}$ sample with 3-5% efficiency. $b\bar{b}$ sample has also been tagged using several event shape variables (neural network technique) and using impact parameter, decay length etc. ($\tau_b \approx 10^{-12}$ sec) from secondary vertex reconstruction.

3.3 Results

A fit has been performed [9] using all measured cross sections, leptonic forward-backward asymmetries and tau polarization data. The fit does not assume lepton universality but gets the value of vector and axial vector couplings of the leptons to Z which are the same for all 3 lepton flavours within the experimental error. The results of the fit are summarized in table and the 1 σ contour is shown in figure 8.

In the charged current sector, lepton universality is examined from accurate measurement of τ lifetime and leptonic branching ratios of the τ lepton. The measurements [10] yield $\tau_\tau =$

Table 1. Axial vector and vector couplings of the charged leptons to Z

	e	μ	τ
g_a	-0.50096 ± 0.00093	-0.5013 ± 0.00123	-0.5005 ± 0.0014
g_v	-0.0373 ± 0.0031	-0.0288 ± 0.0064	-0.0372 ± 0.0032

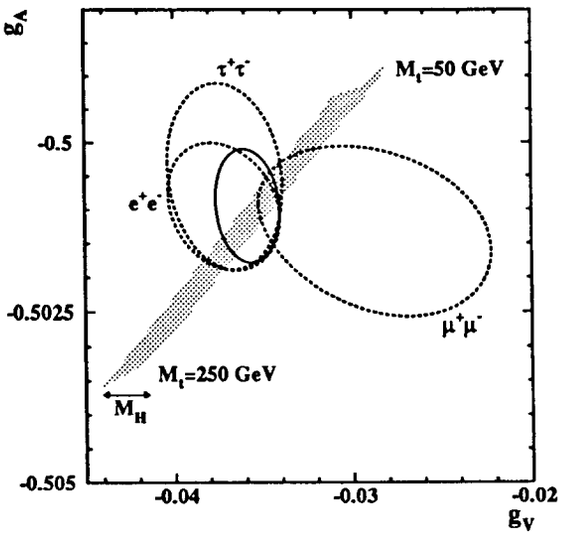

Figure 8: One σ contour plot of g_a vs g_v of the leptons as measured in LEP. The Standard Model prediction is shown as a band on the plot

294.7 ± 3.0 fsec, $B(\tau \to e\nu_\tau\bar{\nu}_e) = 17.89 \pm 0.14$ and $B(\tau \to \mu\nu_\tau\bar{\nu}_\mu) = 17.34 \pm 0.16$. This leads to

$$\frac{g_\tau^W}{g_\mu^W} = 0.999 \pm 0.007 \qquad \frac{g_e^W}{g_\mu^W} = 1.0009 \pm 0.0066$$

Now one can perform a fit to all the data assuming lepton universality. The results of such a fit is summarized in table 2.

Table 2. Z Boson parameters from the fit assuming lepton universality

m_Z	91187 ± 7 MeV
Γ_Z	2489 ± 7 MeV
Γ_{had}	1740.3 ± 5.9 MeV
Γ_{lept}	83.82 ± 0.27 MeV

The measured values of total, hadronic and leptonic widths of Z, leads to the measurement of invisible decay width of Z. From this measurement, one can determine the number of light neutrino families. Using

$$\Gamma_{inv} = 497.6 \pm 4.3 \text{ MeV}$$
$$\text{and } N_\nu = \left(\frac{\Gamma_{inv}}{\Gamma_{lept}}\right)_{meas} \left(\frac{\Gamma_{lept}}{\Gamma_\nu}\right)_{SM}$$

one gets, $N_\nu = 2.980 \pm 0.027$. This method eliminates common systematic errors in the measurement of cross sections and reduces the dependence of top and higgs mass in the standard model calculation. Alternately the process $e^+e^- \to \nu\bar{\nu}\gamma$ has been studied which leads to $N_\nu = 2.80 \pm 0.12$.

All the precision measurements have been compared with the prediction of the Standard Model. With a reasonable range of values of top and Higgs mass, the Standard Model predictions agree with the experimental measurements to better than 0.5%. So a fit has been performed to all data in the framework of the Standard Model. A reasonable fit is obtained for Higgs mass values in the range 60 to 1000 GeV. The results of the fit are summarized in table 3.

Table 3. Estimation of top mass using LEP data

LEP data only	m_{top}	=	$166^{+17\ +19}_{-19\ -22}$ GeV
LEP + other data	m_{top}	=	$164^{+16\ +18}_{-17\ -21}$ GeV

4 α_s Measurements from Event Shape Variables

α_s is determined from relative rate of the two processes $q\bar{q}$ and $q\bar{q}g$. To estimate the relative rate, one uses global event shape variables y which are sensitive to the effect of hard gluon emission.

Fixed order calculations exists [11] upto $\mathcal{O}(\alpha_s^2)$ for all event shape variables. Cumulative cross section R(y) for event shape variable y is given by

$$\begin{aligned} R(y,\alpha_s) &\equiv \int_0^y \frac{1}{\sigma}\frac{d\sigma}{dy} \\ &= \overline{\alpha}_s A(y) + \overline{\alpha}_s^2 \left[B(y) + 2\pi\beta_0 \ln(\mu^2/s) A(y)\right] \end{aligned}$$

with

$$\begin{aligned} \overline{\alpha}_s &= \frac{\alpha_s(\mu)}{2\pi} \\ \beta_0 &= \frac{33 - 2N_f}{12\pi} \end{aligned}$$

A(y), B(y) are computed by integrating $\mathcal{O}(\alpha_s^2)$ ERT matrix elements. This approach describes data well in the multi-jet region, but fails in the two jet region (small y). Recently calculations [12] have been carried out which contain, in addition to the complete $O(\alpha_s^2)$ prediction, the resummation of terms of the form $\alpha_s^n \ln^m y$ (for observable y) with $m \geq n$. Subleading terms of the form $\alpha_s^n \ln^m y$ with $m < n$ are not included beyond the second order ($n > 2$). Calculations exist for thrust ($y \equiv 1 - T$), heavy jet mass ($y \equiv \rho$), energy energy correlation ($y \equiv (1 + \cos\chi)/2$) and average jet multiplicity ($y \equiv y_{cut}$).

The resummed calculations are expected to provide more accurate predictions of the distributions, especially in the kinematic regions where multiple gluon emission is dominant. At the same time, they should have a much reduced dependence on the recombination scale compared to the $O(\alpha_s^2)$ calculations. Both these expectations have been confirmed in several recent experimental studies [13]. Figure 9 shows the QCD fit in comparison with the measured thrust distribution. In all cases a good fit is obtained. The measured α_s values are summarized in table 4.

Table 4. α_s as measured from event topology using resummed calculations

	ALEPH	DELPHI	L3	OPAL	LEP
$\alpha_s(m_Z)$	0.125±0.005	0.123±0.006	0.124±0.008	0.120±0.006	0.123±0.006

5 Search for Higgs Boson

In the Standard Model the Z and $W^{\pm}$ bosons acquire mass through the Higgs mechanism [14], which, in its minimal formulation, predicts the existence of one neutral scalar boson H^0. The H^0 couplings to vector bosons are fixed by gauge invariance and its couplings to fermions are determined by the Yukawa interactions. There is only one free parameter in the model which is chosen to be the mass of the scalar boson. If the Higgs boson is lighter than the Z, it can be produced in Z decays through the bremsstrahlung process [15]:

$$e^+e^- \rightarrow Z \rightarrow H^0 + Z^* \rightarrow H^0 + f\bar{f}$$

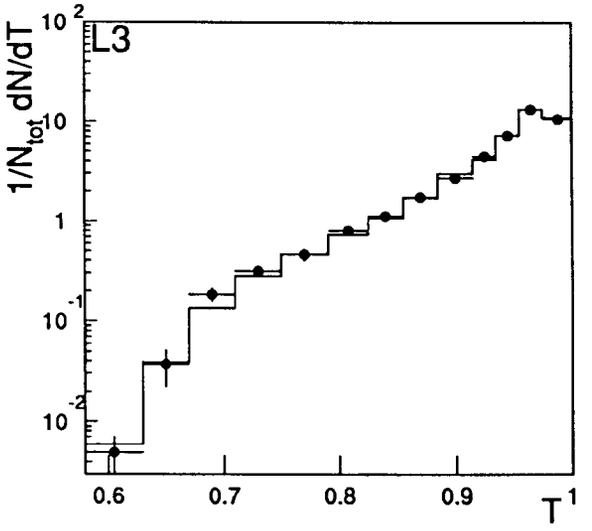

Figure 9: Distribution of the event thrust T compared to the resummed calculation

This will be the dominant production mechanism for a light Higgs in LEP. In the Standard Model the cross section for this process is known as a function of the Higgs mass:

$$\frac{1}{\Gamma(Z \to f\bar{f})}\frac{d\Gamma(Z \to H^0 f\bar{f})}{dx} = \frac{\alpha}{4\pi \sin^2\theta_W \cos^2\theta_W}\frac{\left(1 - x + \frac{x^2}{12} + \frac{2\gamma^2}{3}\right)(x^2 - 4\gamma^2)^{\frac{1}{2}}}{(x-\gamma^2)^2 + \frac{\Gamma_Z}{m_Z}^2}$$

$$\text{with } x = \frac{2E_{H^0}}{m_Z}$$

$$\gamma = \frac{m_H}{m_Z}$$

$$E_{Ho} = \frac{m_Z^2 + m_H^2 - m_{f\bar{f}}^2}{2m_Z}$$

Higher order electroweak corrections have been taken into account using the improved Born approximation and accounting for radiative corrections to the ZZ^*H^0 vertex. The vertex correction reduces top mass dependence in the production rate of H^0. The effect of initial state photon radiation has been computed using an exponentiation technique. Figure 10 shows the rate of production as a function of Higgs mass together with the rate of Higgs production through Z decaying to $H^0\gamma$. It is evident from the figure that associate production with $f\bar{f}$ is a more promising channel for direct H^0 search over a large range of m_H.

Higgs decay is controlled by the Yukawa couplings and the decays to the heaviest possible fermion pair is favoured. The decay partial width is given by [16]

$$\Gamma(H^0 \to f\bar{f}) = \frac{N_C g^2 m_f^2 m_H}{32\pi m_W^2}\beta_f^3$$

$$\text{with } \beta_f = \sqrt{1 - \frac{4m_f^2}{m_H^2}}$$

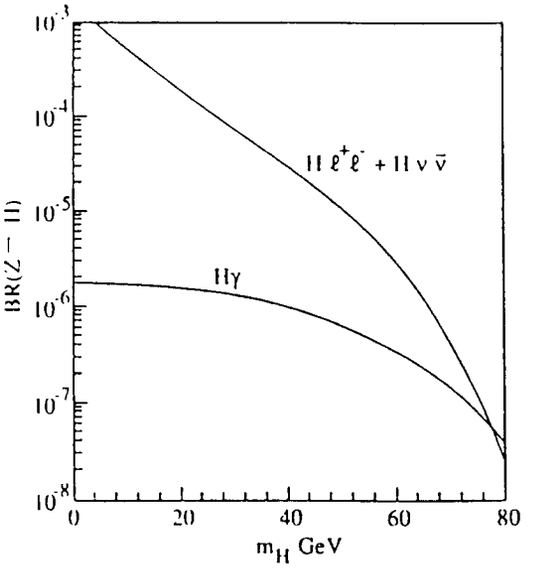

Figure 10: Expected branching fraction for Z decaying to Standard Model Higgs

As a result of the Yukawa coupling, the Higgs width increases very rapidly with Higgs mass. The Higgs decays predominantly into $b\bar{b}$ for masses above 11 GeV, although the branching ratios into $c\bar{c}$ and $\tau^+\tau^-$ are not negligible. In the mass range from 4 to 11 GeV, decays into $\tau^+\tau^-$ and $c\bar{c}$ dominate. Between $2m_\mu$ and $c\bar{c}$ threshold, Higgs dominantly decay to light quarks or to a pair of gluons via a heavy quark in the loop. Below 2 GeV non-perturbative effects make the prediction of the branching ratios less firm. In this last region, the experimental Higgs search should be independent of the decay modes. Below the $2m_\mu$ threshold the Higgs can decay only into two electrons or two photons. In this case the Higgs width is very small and consequently its lifetime can be so long that it can decay outside the detector.

The search criteria are chosen differently for different Higgs mass range. No evidence of Higgs boson has been observed in all the searches carried out so far. The different experiments have given 95% confidence level lower limit to the Higgs mass as summarized in table 5.

Table 5. 95% CL lower limit on m_H

ALEPH	DELPHI	L3	OPAL	LEP
58.4 GeV	54.7 GeV	57.7 GeV	57.5 GeV	63.5 GeV

6 Summary

LEP has accumulated 5 million Z in the year 1991 and 1992. The precision data have resulted in an accurate determination of the electroweak parameters and the strong coupling constant.

m_Z	=	91187 ± 7 MeV	$g_{a\ell}$	=	−0.50093 ± 0.00082
Γ_Z	=	2489 ± 7 MeV	$g_{v\ell}$	=	−0.0359 ± 0.0018
$\Gamma_{b\bar{b}}/\Gamma_{had}$	=	0.2200 ± 0.0027	$\sin^2\theta_{eff}$	=	0.2324 ± 0.0005

Lepton universality has been tested at 0.3% level in the neutral current sector and at 0.7% level in the charged current sector. Number of light ν families has been determined to be $N_\nu = 2.980 \pm 0.027$ from indirect measurements and $N_\nu = 2.80 \pm 0.12$ from direct measurements.

All measurements are in excellent agreement with the standard model expectations. Standard model has been tested at $\sim 0.5\%$ level using these measurements. There is indirect evidence of top quark from measurement of I_3^b. All data are consistent with the Standard Model with top mass, $m_{top} = 166^{+17}_{-19}\ ^{+19}_{-22}$ GeV.

No evidence of any new particle or new physics has been seen as yet. Standard Model Higgs boson with mass smaller than 63.5 GeV has been ruled out.

Additional ~ 3 million Z events have been recorded at LEP during 1993. This will improve the precision of the electroweak parameters significantly and improve the searches in near future.

References

[1] C. Rubbia, P. McIntyre and D. Cline, Proc. Int. Neutrino Conference, Aachen (1976) 683.

[2] UA1 Collaboration, G. Arnison *et al.*, Phys. Lett. **B122** (1983) 106;
UA2 Collaboration, M. Banner *et al.*, Phys. Lett. **B122** (1983) 476.

[3] C. Rubbia, Nobel Lecture (1984) 54.

[4] S.L. Glashow, Nucl. Phys. **22** (1961) 579;
S. Weinberg, Phys. Rev. Lett. **19** (1967) 1264;
A. Salam, "Elementary Particle Theory", Ed. N. Svartholm, Stockholm, "Almquist and Wiksell" (1968), 367.

[5] UA1 Collaboration, G. Arnison *et al.*, Phys. Lett. **B126** (1983) 398;
UA2 Collaboration, M. Banner *et al.*, Phys. Lett. **B129** (1983) 150.

[6] C. Camilleri *et al.*, Physics with very high energy e^+e^- colliding beams, CERN/76-18, CERN, 1976;
M. Bourquin *et al.*, Preprint 86-02.

[7] M. Consoli and W. Hollik, Z Physics at LEP 1, CERN report CERN 89-08, Vol.1, page 7, eds. G. Altarelli *et al.*;
G. Burgers and F. Jegerlehner: Z Physics at LEP 1, CERN report CERN 89-08, Vol.1, page 55, eds. G. Altarelli *et al.*;
F. Berends: Z Physics at LEP 1, CERN report CERN 89-08, Vol.1, page 89, eds. G. Altarelli *et al.*;
M. Caffo, E. Remiddi:: Z Physics at LEP 1, CERN report CERN 89-08, Vol.1, page 171, eds. G. Altarelli *et al.*;
M. Böhm and W. Hollik: Z Physics at LEP 1, CERN report CERN 89-08, Vol.1, page 203, eds. G. Altarelli *et al.*;
S. Jadach and Z. Was: Z Physics at LEP 1, CERN report CERN 89-08, Vol.1, page 235, eds. G. Altarelli *et al.*;
J.H. Kühn and P.M. Zerwas: Z Physics at LEP 1, CERN report CERN 89-08, Vol.1, page 267, eds. G. Altarelli *et al.*.

[8] S. Jadach and Z. Was, Z Physics at LEP 1, CERN report CERN 89-08, Vol.1, page 235, eds. G.Altarelli *et al.*.

[9] The LEP Collaborations ALEPH, DELPHI, L3, OPAL and the LEP Electroweak Working Group, CERN-PPE/93-157.

[10] A. Schwarz, Lepton Photon Conference, Cornell (1993).

[11] Z. Kunszt and P. Nason, Z Physics at LEP 1, CERN report CERN 89-08, Vol.1, page 373, eds. G. Altarelli *et al.*.

[12] S. Catani *et al.*, Phys. Lett. **B269** (1991) 432;
S. Catani, Proc 17th Workshop on the INFN Eloisatron Project, Erice, June 1991;
S. Catani *et al.*, Phys. Lett. **B263** (1991) 491;
S. Catani *et al.*, Phys. Lett. **B272** (1991) 368;
G. Turncock, Cavendish-HEP-92-3.

[13] ALEPH Collaboration, D. Decamp *et al.*, Phys. Lett. **B284** (1992) 163;
DELPHI Collaboration, P. Abreu *et al.*, CERN-PPE/93-43;
L3 Collaboration, O. Adriani *et al.*, Phys. Lett. **B284** (1992) 471;
OPAL Collaboration, P.D. Acton *et al.*, CERN-PPE/93-38.

[14] P.W. Higgs, Phys. Lett. **12** (1964) 132; Phys. Rev. Lett. **13** (1964) 508; Phys. Rev. Lett. **145** (1966) 1156;
F. Englert and R. Brout, Phys. Rev. Lett. **13** (1964) 321.

[15] B.L. Ioffe, V.A. Khoze, Sov. J. Part. Nucl. **9** (1978) 50;
J.D. Bjorken, SLAC-PUB-1866 (1977) 1;
J. Finford, Phys. Scripta **21** (1980) 143.

[16] P. Franzini *et al.*, Z Physics at LEP 1, CERN report CERN 89-08, Vol.2, page 59, eds. G. Altarelli *et al.*.